

755 Supplementary Materials

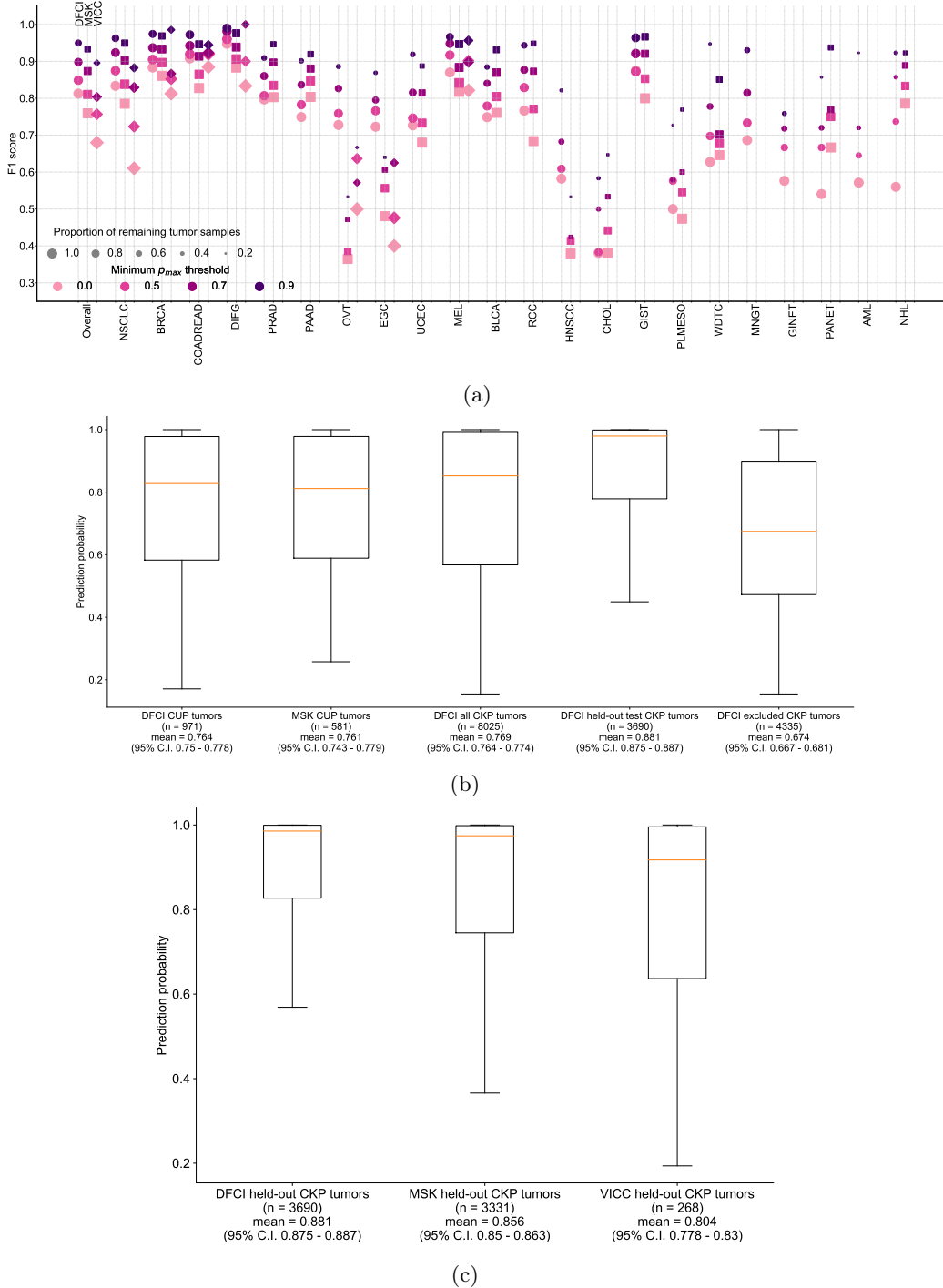


Figure S1

Figure S1: **OncoNPC prediction performances and confidences (i.e., p_{\max}) across chosen cohorts and centers.** (a) Center-specific OncoNPC performance (in weighted F1) on the test CKP tumor samples ($n = 7,289$). The figure is a breakdown of Fig. 2c based on cancer center (DFCI: \circ , MSK: \square , VICC: \diamond). The performance was evaluated at 4 different prediction confidences (i.e., minimum p_{\max} thresholds). Each dot size is scaled by the proportion of tumor samples retained. See Table S1 for the center-specific number of test CKP tumor samples broken down by cancer types and prediction confidence thresholds. (b), (c) Box plots of prediction confidences (p_{\max}) across (b) DFCI CUP tumors, MSK CUP tumors, all DFCI CKP tumors, DFCI held-out CKP tumors, and DFCI excluded CKP tumors, and (c) DFCI held-out CKP tumors, MSK held-out CKP tumors, and VICC held-out CKP tumors. The figures display medians, lower and upper quartiles, as well as the mean and 95% confidence intervals, along with the number of tumor samples.

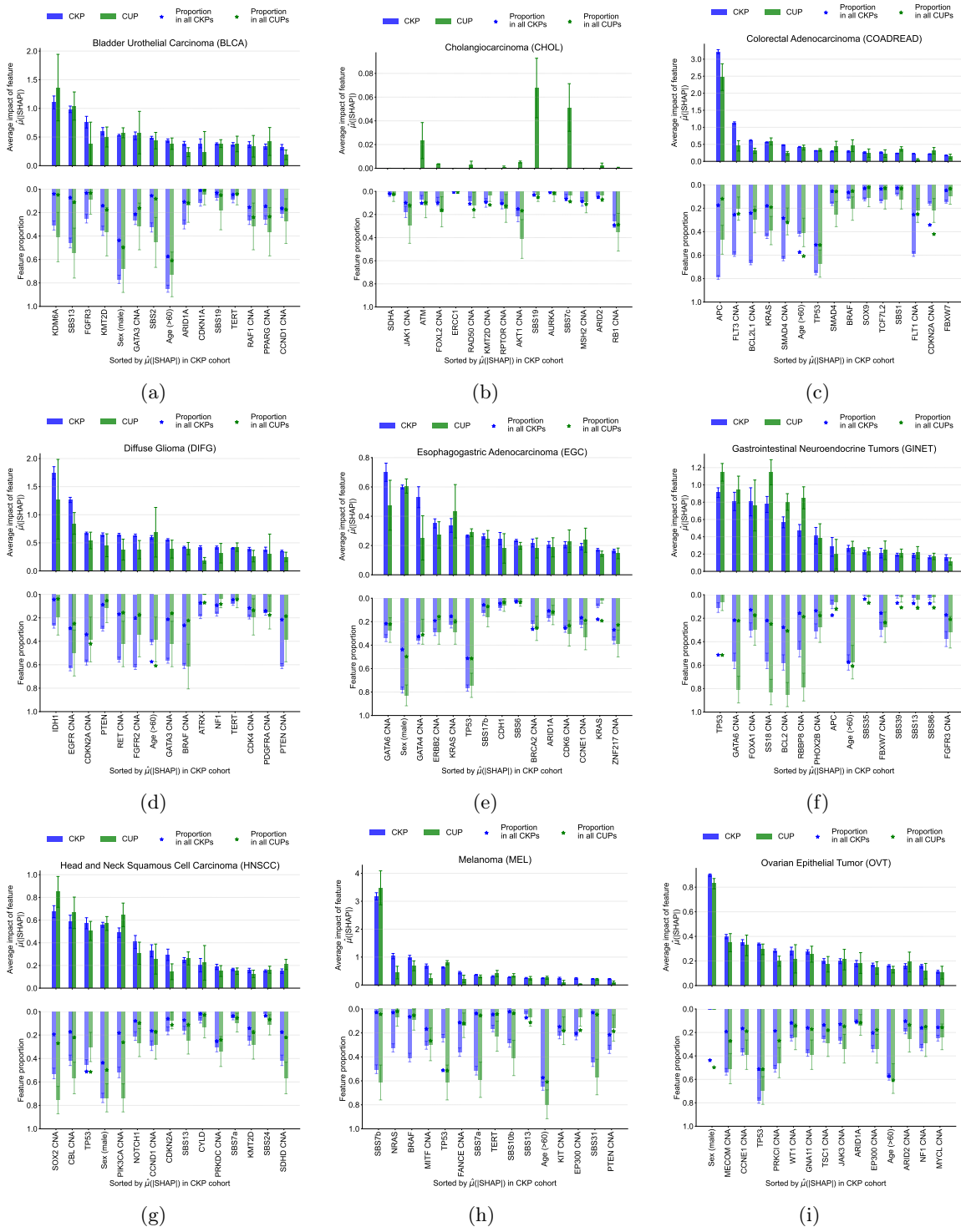


Figure S2

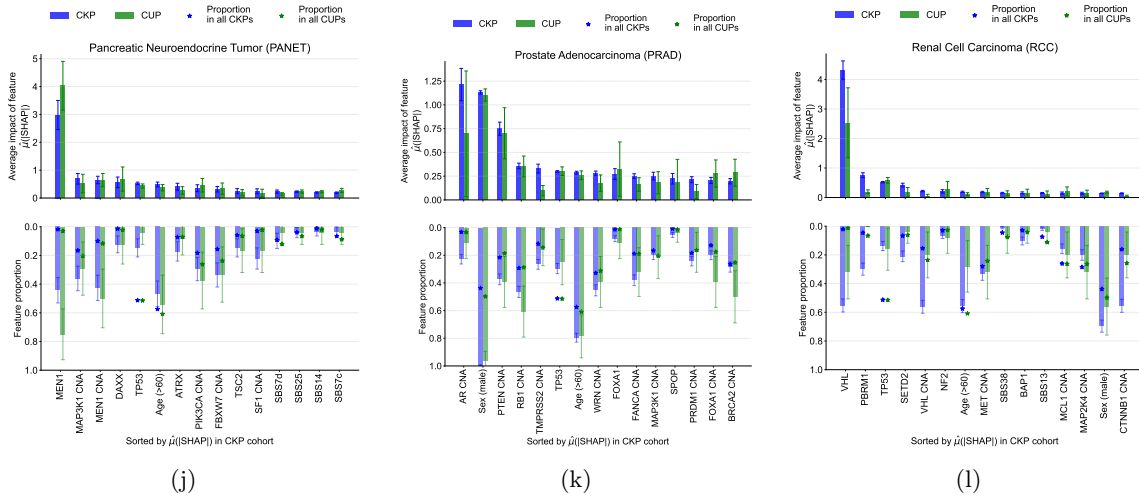


Figure S2: Interpreting OncoNPC predictions. Top 15 most important features, based on mean absolute SHAP values (i.e., $\hat{\mu}(|\text{SHAP}|)$ [19]), for cancer types with at least 20 CUP tumors samples were classified.

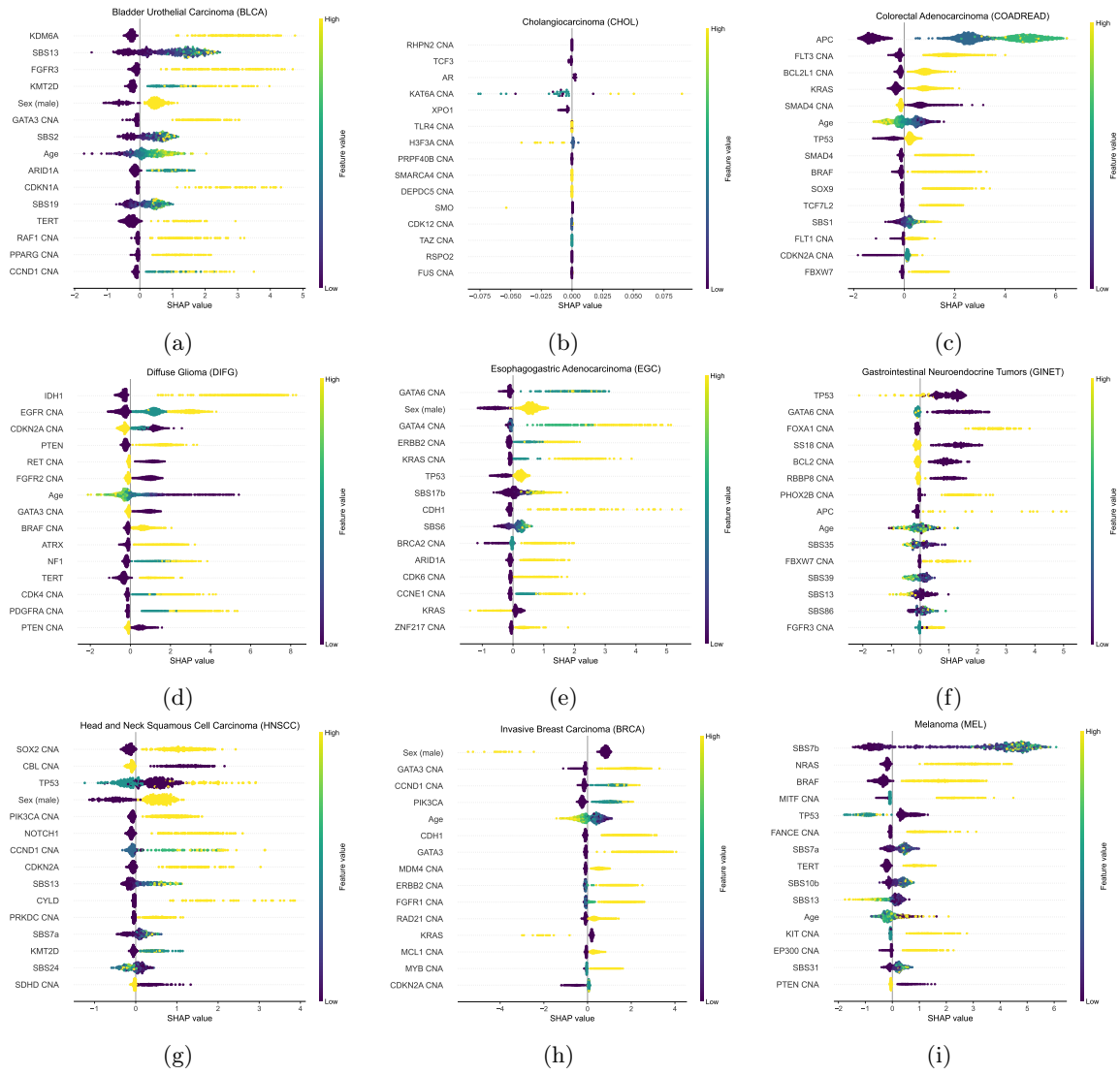


Figure S3

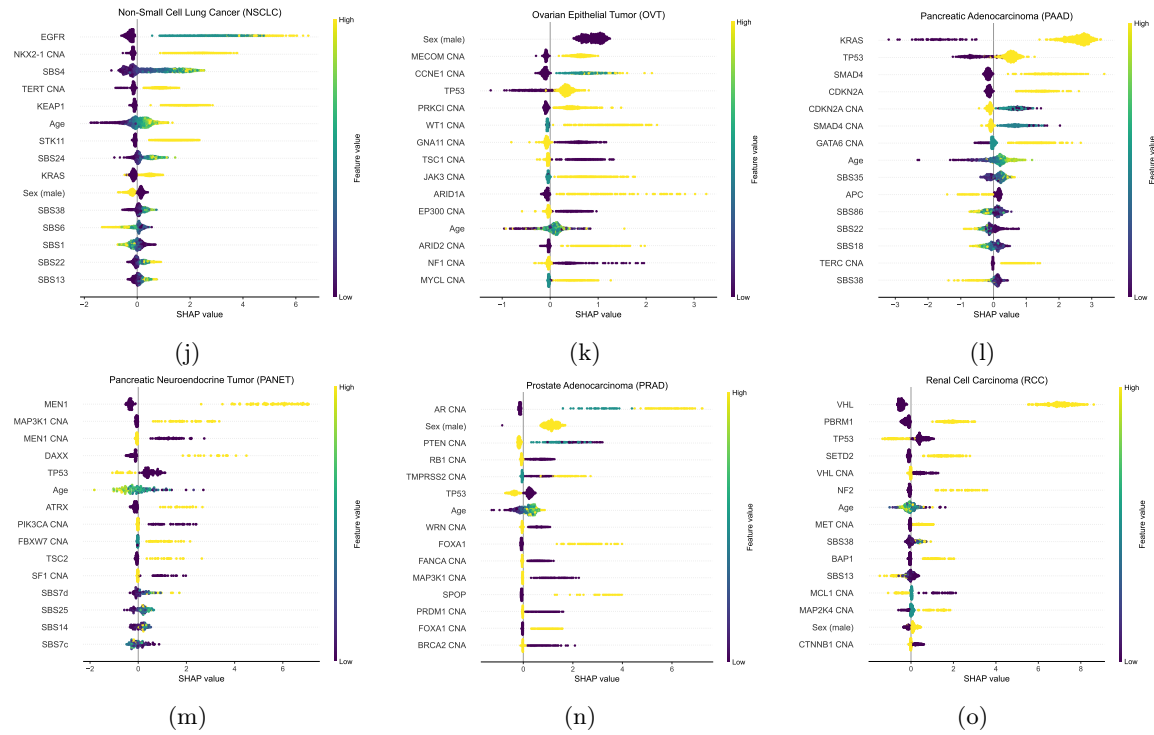


Figure S3: **SHAP summary plot** [19] for cancer types with at least 20 CUP tumors samples were classified. SHAP values (i.e., impact on OncoNPC predictions) are shown on the x-axis, while feature values are shown as a color map (from purple to yellow). In each plot, CUP and CKP tumor samples were combined into a single cohort for the corresponding cancer.

Predicted cancer type : Non-Small Cell Lung Cancer (NSCLC)
 Posterior probability : 0.98

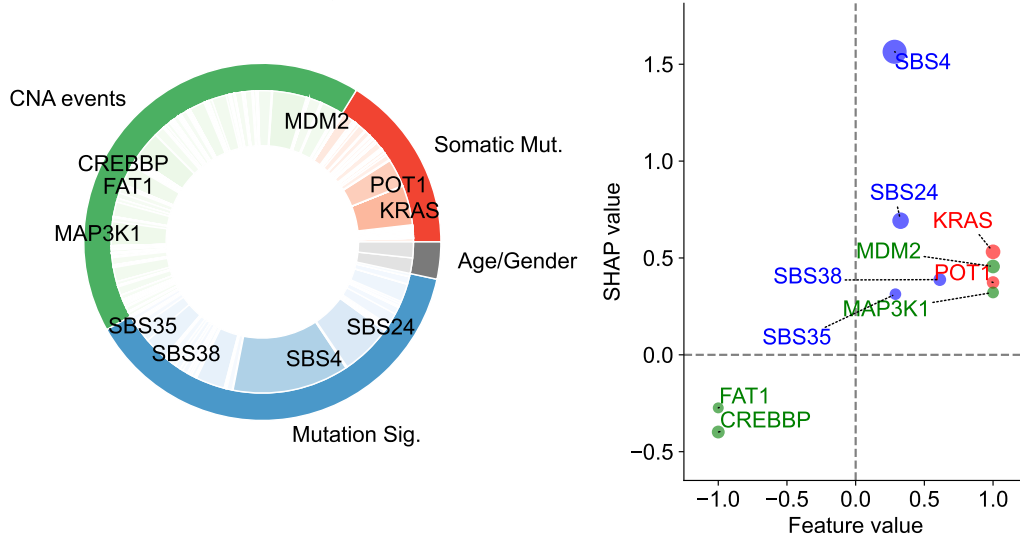


Figure S4: **Explanation of OncoNPC prediction for a patient with CUP.** The patient is a 76 year-old male, with a tumor biopsy from the liver. The pie chart on the left shows the Top 10 important features across three different feature categories (i.e., CNA events, somatic mutation, and mutation signatures), and the scatter plot on the right shows their SHAP values and feature values. The size of each dot is scaled by corresponding absolute SHAP value. From the chart review, we found that the patient reported a 60-pack year smoking history, as well as having lived near a tar and chemical factory as a child. Despite the CUP diagnosis, OncoNPC confidently classified the primary site as NSCLC with posterior probability of 0.98. SBS4, a tobacco smoking-associated mutation signature, was significantly enriched in the patient's tumor sample, which has, by far, the most impact on the prediction; followed by SBS24 mutation signature associated with known exposures to aflatoxin [20]; and KRAS mutation. Note that inhalation of aflatoxin has been linked to cause primary lung cancer [60–62], and KRAS mutation is one of the most common drivers of NSCLC [63, 64].

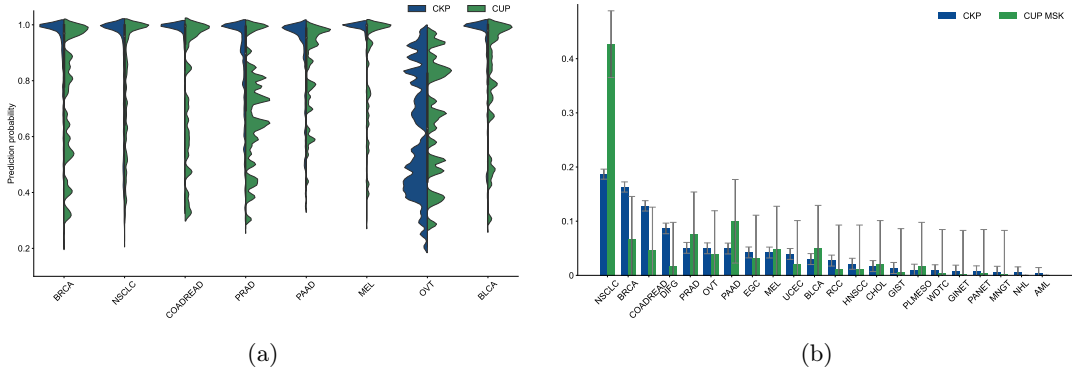


Figure S5: Applying OncoNPC to MSK CUP tumor samples. (a) Empirical distributions of prediction probabilities for correctly predicted held-out CKP tumor samples ($n = 3,429$) and MSK CUP tumor samples ($n = 496$), broken down by CKP cancer types (blue) and their corresponding OncoNPC predicted cancer types for CUP tumors (green). Only OncoNPC classifications with at least 20 CUP tumor samples are shown. (b) Proportion of each CKP cancer type and the corresponding OncoNPC predicted CUP cancer type. All training CKP tumor samples ($n = 36,445$) and all MSK CUP tumor samples ($n = 581$) are shown. For both (a) and (b), the cancer types (x-axis) are ordered by the number of CKP tumor samples in each cancer type

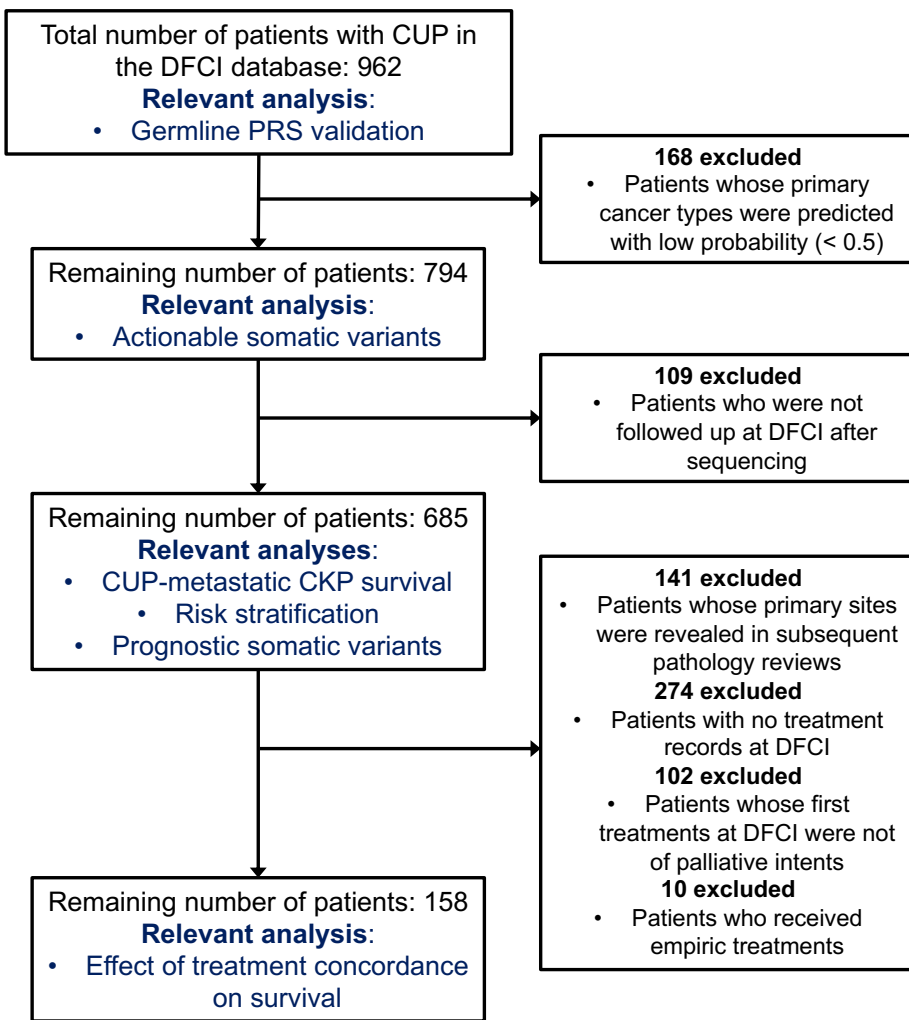


Figure S6: Exclusion criteria for downstream clinical analyses.

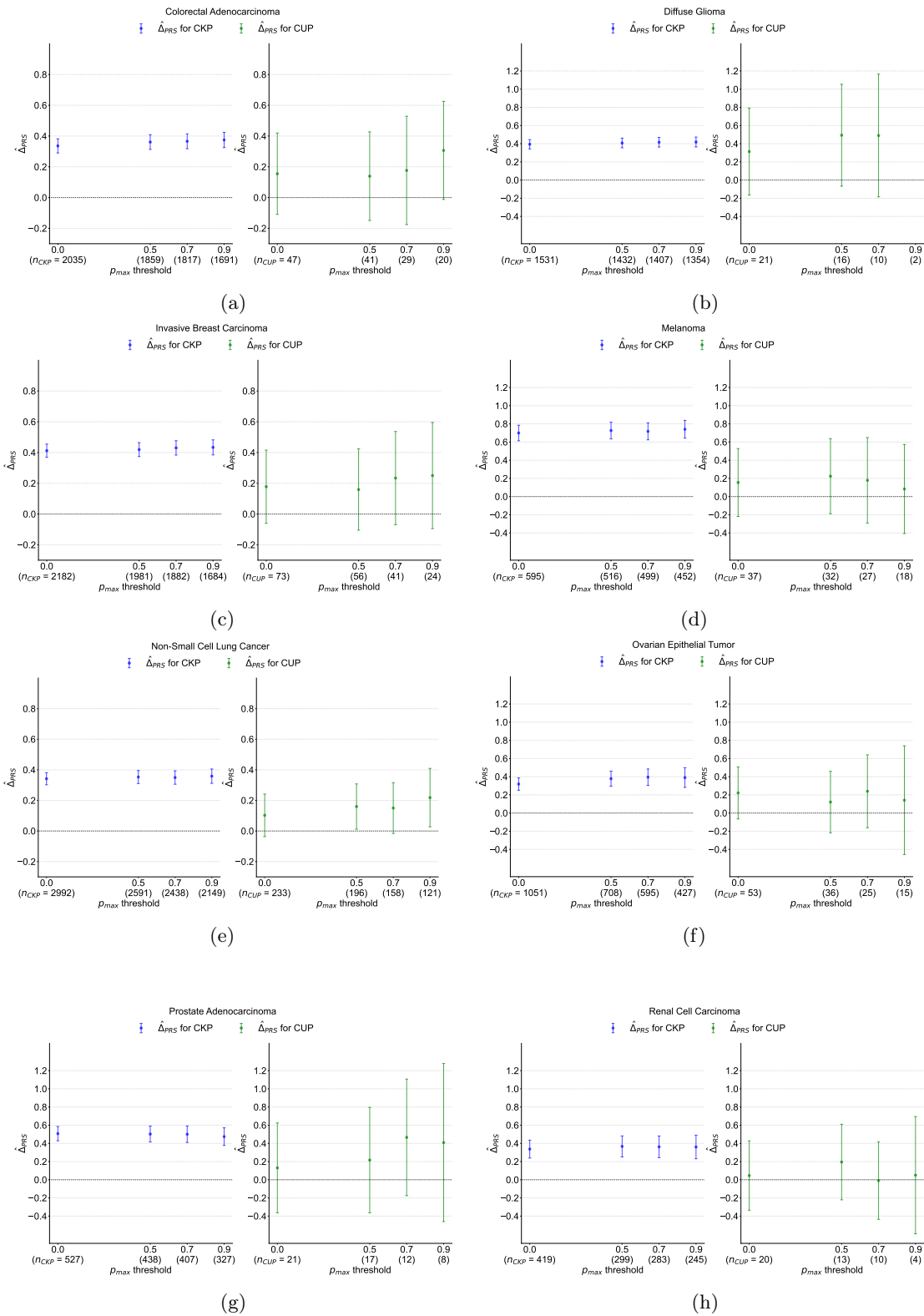


Figure S7

Figure S7: Germline Polygenic Risk Score (PRS) enrichment of CKP tumor samples and CUP tumor samples, broken down by 8 different cancer types: (a) Colorectal Adenocarcinoma (COADREAD), (b) Diffuse Glioma (DIFG), (c) Invasive Breast Carcinoma (BRCA), (d) Melanoma (MEL), (e) Non-Small Cell Lung Cancer (NSCLC), (f) Ovarian Epithelial Tumor (OVT), (g) Prostate Adenocarcinoma (PRAD), and (h) Renal Cell Carcinoma (RCC). The magnitude of the enrichment is quantified by $\hat{\Delta}_{\text{PRS}}$: the mean difference between the concordant (i.e. OncoNPC matching) cancer type PRS and mean of PRSs of discordant cancer types (see Methods). $\hat{\Delta}_{\text{PRS}}$ is shown for CKPs in blue (for reference) and CUPs in green.

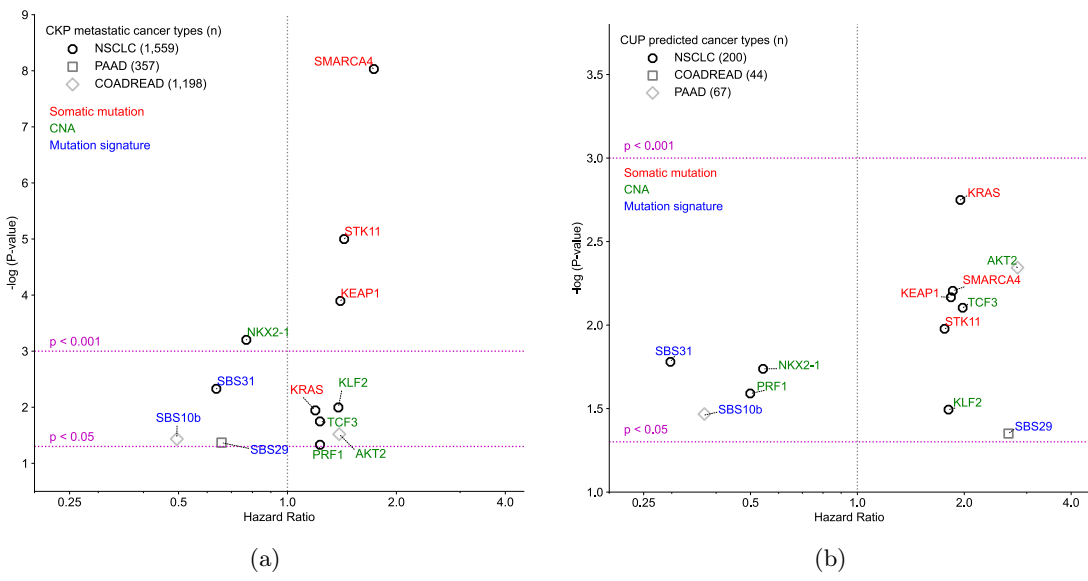


Figure S8: Prognostic biomarkers between OncoNPC classifications and known cancers.
(a), (b) Prognostic somatic variants significantly associated with overall survival, shared between three different CUP **(a)**-metastatic CKP **(b)** pairs (NSCLC, PAAD, and COADREAD; indicated by point shape). Variant types are indicated by colors: red for somatic mutations, green for CNAs, and blue for mutation signatures.

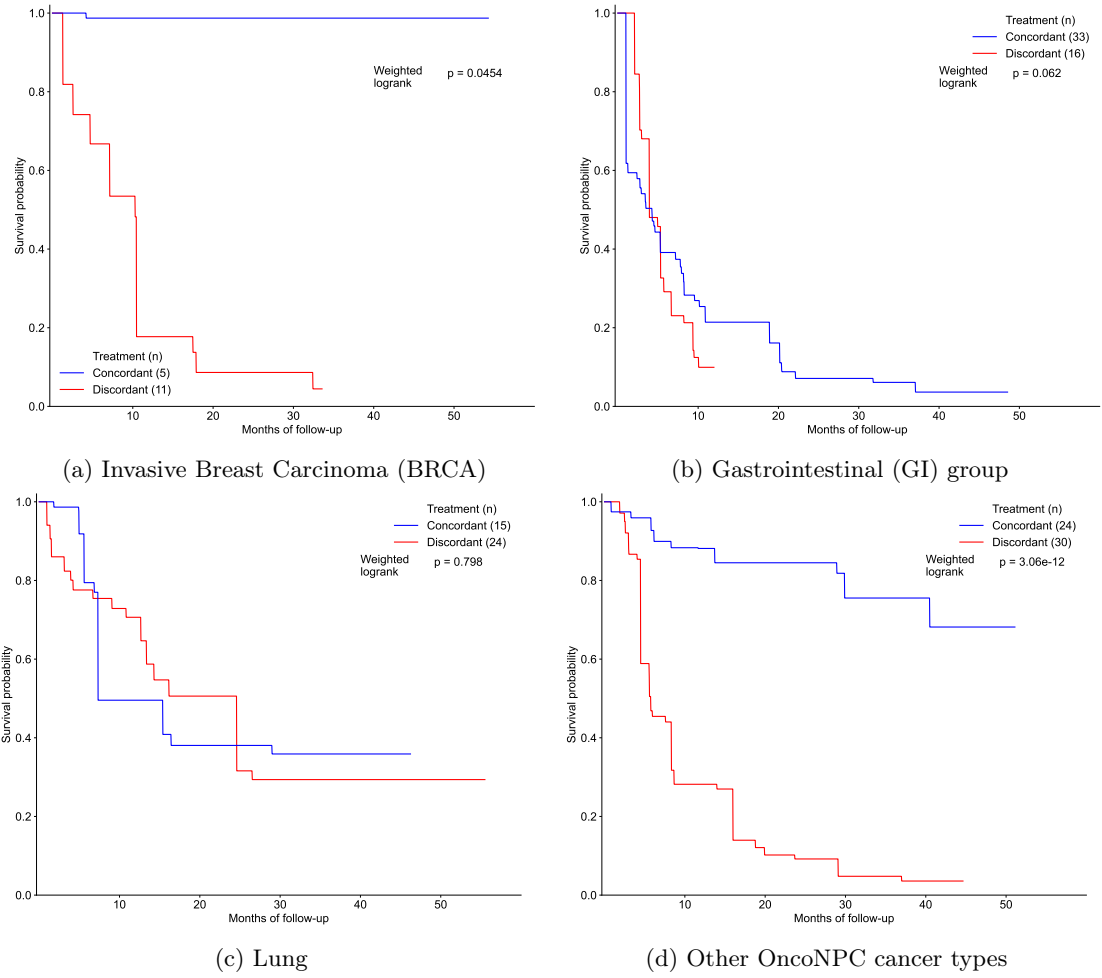


Figure S9: Estimated survival curves for patients with CUP, broken down by OncoNPC predicted cancer types: (a) BRCA, (b) Gastrointestinal (GI) group (CHOL, COADREAD, EGC, and PAAD), (c) Lung (NSCLC and PLMESO), and (d) other OncoNPC cancer types (BLCA, DIFG, GINET, HNSCC, MEL, OVT, PANET, PRAD, RCC, and UCEC). In each figure, the concordant treatment group and discordant treatment group are shown in blue and red, respectively. To estimate the survival function for each group, we utilized Inverse Probability of Treatment Weighted (IPTW) Kaplan-Meier estimator while adjusting for left truncation until time of sequencing (see Methods). Statistical significance of the survival difference between the two groups was estimated by a weighted log-rank test [59].

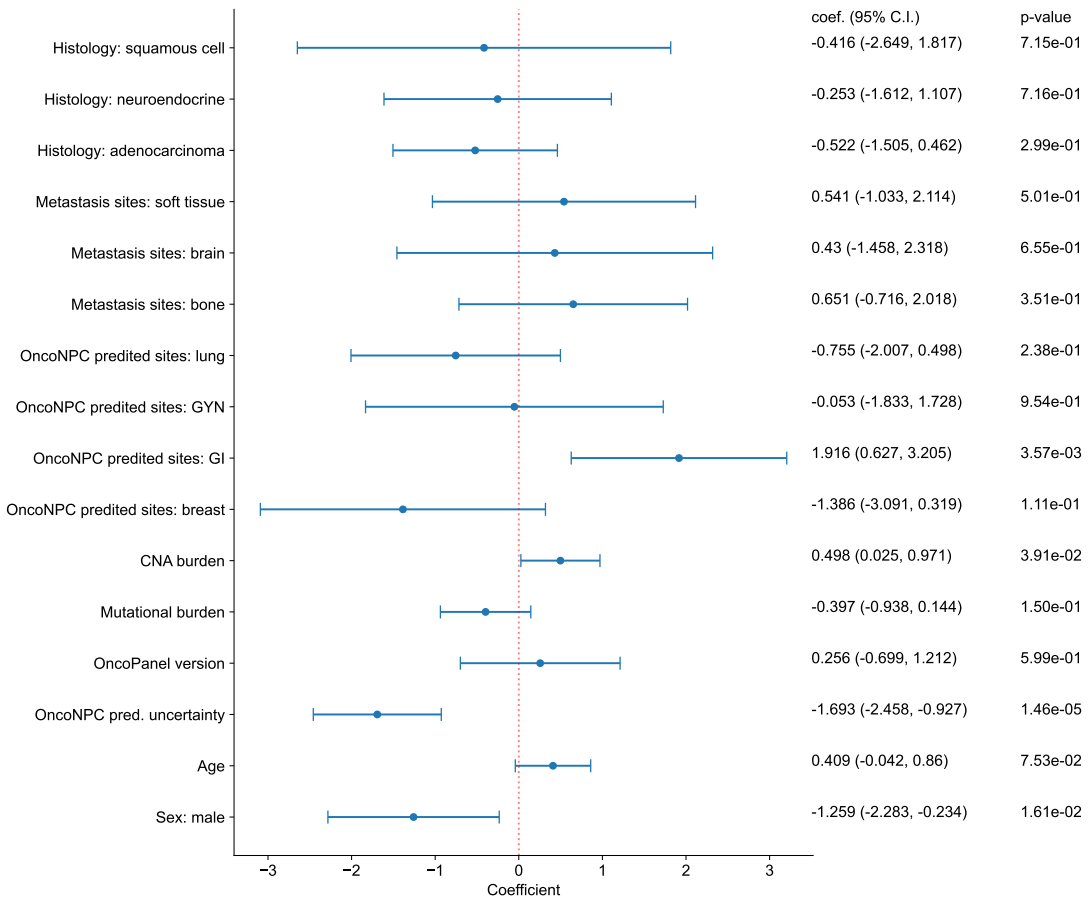


Figure S10: Summary of coefficients for estimating treatment-OncoNPC concordance. Formally, we estimated out-of-sample $P(A|X)$, where A corresponds to the treatment-OncoNPC concordance, using a logistic regression model in a 10-fold cross-fitting. The coefficients were obtained from the first fold. See Methods.

Table S1: Center-specific number of held-out CKP tumor samples, broken down by cancer types and prediction confidence (i.e., p_{\max}) thresholds.

		Minimum p_{\max} threshold						Minimum p_{\max} threshold			
		0.0	0.5	0.7	0.9			0.0	0.5	0.7	0.9
Overall	DFCI	3690	3438	3047	2502	Renal Cell Carcinoma (RCC)	DFCI	79	71	61	50
	MSK	3331	3012	2608	2112		MSK	85	75	68	56
	VICC	268	230	192	136		VICC	6	5	4	3
Non-Small Cell Lung Cancer (NSCLC)	DFCI	811	735	644	533	Head and Neck Squamous Cell Carcinoma (HNSCC)	DFCI	55	50	39	28
	MSK	717	618	520	430		MSK	27	18	12	5
	VICC	36	27	23	19		VICC
Invasive Breast Carcinoma (BRCA)	DFCI	600	572	514	433	Cholangiocarcinoma (CHOL)	DFCI	18	12	10	7
	MSK	727	675	598	474		MSK	40	31	24	16
	VICC	68	62	48	35		VICC	1	.	.	.
Colorectal Adenocarcinoma (COADREAD)	DFCI	521	502	479	436	Gastrointestinal Stromal Tumor (GIST)	DFCI	47	46	43	40
	MSK	375	358	330	303		MSK	34	33	31	30
	VICC	55	52	48	37		VICC
Diffuse Glioma (DIFG)	DFCI	400	390	383	361	Well-Differentiated Thyroid Cancer (WDTC)	DFCI	17	15	14	9
	MSK	214	204	187	168		MSK	31	31	29	25
	VICC	11	10	8	4		VICC	1	1	1	.
Prostate Adenocarcinoma (PRAD)	DFCI	126	118	98	67	Pleural Mesothelioma (PLMESO)	DFCI	24	21	14	10
	MSK	300	280	233	163		MSK	18	17	10	6
	VICC	16	10	6	3		VICC	5	3	2	1
Pancreatic Adenocarcinoma (PAAD)	DFCI	136	125	104	71	Meningothelial Tumor (MNGT)	DFCI	27	25	23	20
	MSK	233	216	187	154		MSK	3	3	1	.
	VICC	10	8	6	1		VICC	1	1	1	1
Ovarian Epithelial Tumor (OVT)	DFCI	257	229	184	112	Gastrointestinal Neuroendocrine Tumors (GINET)	DFCI	20	17	16	11
	MSK	100	60	38	10		MSK	3	3	2	.
	VICC	12	9	5	2		VICC
Esophagogastric Adenocarcinoma (EGC)	DFCI	171	153	114	66	Pancreatic Neuroendocrine Tumor (PANET)	DFCI	15	14	13	8
	MSK	82	70	44	24		MSK	24	22	19	15
	VICC	11	8	7	2		VICC
Endometrial Carcinoma (UCEC)	DFCI	123	116	95	73	Acute Myeloid Leukemia (AML)	DFCI	15	11	10	6
	MSK	105	100	91	70		MSK
	VICC	7	6	6	2		VICC
Melanoma (MEL)	DFCI	134	127	115	103	Non-Hodgkin Lymphoma (NHL)	DFCI	8	8	7	6
	MSK	108	103	98	92		MSK	12	11	8	6
	VICC	24	24	23	23		VICC
Bladder Urothelial Carcinoma (BLCA)	DFCI	86	81	67	52						
	MSK	93	84	78	65						
	VICC	4	4	4	3						

756 **Supplementary Notes**

757 **Identifying prognostic somatic variants shared in CUP-metastatic CKP
758 pairs**

759 To identify prognostic somatic variants shared between CUP/metastatic-CKP pairs, we again re-
760 stricted to the 7 common OncoNPC subtypes with at least 35 CUP patients: NSCLC, PAAD,
761 BRCA, COADREAD, HNSCC, EGC, GINET, and OVT. For somatic variants, we utilized the same
762 processed features utilized in the OncoNPC model training (see Methods: Feature selection and
763 OncoNPC model interpretation). To ensure sufficient statistical power, we restricted to candidate
764 somatic variants (i.e., mutated genes and CNA genes) present in at least 15 samples in a given On-
765 coNPC subtype and corresponding metastatic CKP cohort, as well as all 96 mutational signatures.

766 After selecting the cancer types to consider in the CUP-metastatic CKP pairs and candidate
767 somatic variants for each pair, we iteratively tested each feature for association with survival in
768 each OncoNPC subtype and in each corresponding metastatic CKP cohort. A multivariable Cox
769 Proportional Hazard regression [32] model was used with time-to-death from sequencing as the
770 outcome. To adjust for baseline effects, we included age at sequencing, sex, tumor sequencing panel
771 version, mutational burden (i.e., sum of total somatic mutations in each tumor sample), and CNA
772 burden (i.e., sum of total CNA events in each tumor sample) as covariates. Finally, to identify
773 shared prognostic somatic variants for each CUP-metastatic CKP pair, we retained somatic variants
774 which passed Schoenfield residuals-based proportional hazard tests (Python `lifelines` v0.27.4 [65]:
775 p-value threshold: 0.05) and were nominally significant ($p < 0.05$) for both CUP and CKP cancer
776 types in each pair.

777 Three out of 14 tested CUP-metastatic CKP pairs (NSCLC, PAAD, and COADREAD) exhibited
778 shared prognostic somatic variants significantly associated with overall survival with nominal p-value
779 cut-off at 0.05 (Fig. S8a and S8b). In patients with known or classified NSCLC, three somatic
780 mutations were associated with poor survival in both groups: SMARCA4 (CUP: H.R. 1.86, 95%
781 C.I. 1.19 - 2.89, p-value 6.23×10^{-3} , CKP mets: H.R. 1.73, 95% C.I. 1.44 - 2.09, p-value 9.30×10^{-9}),
782 STK11 (CUP: H.R. 1.76, 95% C.I. 1.14 - 2.71, p-value 1.05×10^{-2} , CKP mets: H.R. 1.43, 95% C.I. 1.22
783 - 1.68, p-value 1.00×10^{-5}), and KEAP1 (CUP: H.R. 1.83, 95% C.I. 1.18 - 2.85, p-value 6.82×10^{-3} ,
784 CKP mets: H.R. 1.40, 95% C.I. 1.18 - 1.66, p-value 1.27×10^{-4}). These associations of somatic
785 mutations in SMARCA4, STK11, and KEAP1 genes with overall survival are well established for
786 NSCLC [66–68]. Interestingly, a CNA event in NKX2-1 was associated with improved survival in the
787 patients from the NSCLC pair (CUP: H.R. 0.542, 95% C.I. 0.326 - 0.901, p-value 1.83×10^{-2} , CKP
788 mets: H.R. 0.770, 95% C.I. 0.662 - 0.894, p-value 6.28×10^{-4}), consistent with prior meta-analyses
789 [69]. In patients with known or classified COADREAD tumors, SBS10b mutation signature, linked
790 to polymerase epsilon exonuclease domain mutations [20], was associated with longer overall survival
791 (CUP: H.R. 0.371, 95% C.I. 0.148 - 0.928, p-value 3.41×10^{-2} , CKP mets: H.R. 0.495, 95% C.I.
792 0.255 - 0.958, p-value 3.68×10^{-2}). Finally, in patients with known or classified PAAD tumors,
793 the SBS29 mutation signature (commonly found in tumor samples from individuals with a tobacco
794 chewing habit [20]) was associated with poor survival in CUPs but nominally protective in metastatic

795 CKPs (CUP: H.R. 2.66, 95% C.I. 1.02 - 6.93, p-value 4.46×10^{-2} , CKP mets: H.R. 0.657, 95% C.I.
796 0.438 - 0.986, p-value 4.28×10^{-2}). Although these somatic associations remain to be validated in
797 independent cohorts, by categorizing patients with CUP based on their OncoNPC predictions, we
798 were able to identify prognostic somatic variants, consistent with recent research findings.

799 **Determining treatment-OncoNPC concordance**

800 Concordance of OncoNPC predicted cancer type with a first palliative treatment assignments at
801 DFCI was classified in one of five categories: 1) “TRUE”: the OncoNPC cancer type matched
802 the clinically proven/suspected tumor type and the predicted treatment matched the treatment
803 received, which was dictated by NCCN guidelines and/or standard of care, within the clinical context
804 provided by the medical record; 2) “FALSE”: the OncoNPC cancer type did not match the clinically
805 proven/suspected cancer type and the predicted treatment was not appropriate per NCCN guidelines
806 or standard of care, in most reasonable situations, and within the context of the medical record; 3)
807 “SOFT FALSE”: the OncoNPC cancer type did not match the clinically proven/suspected cancer
808 type, but the treatment received was not chosen based on NCCN guidelines or standard of care, owing
809 to the unique clinical context provided by the medical record, 4) “EMPIRIC”: treatment received was
810 empiric treatment for cancer of unknown primary (e.g., carboplatin/taxol or gemcitabine/cisplatin)
811 with the corresponding clinical rationale; in cases where patients received these regimens but not
812 with the clinical intent of empiric CUP treatment (i.e., as regimens intended for treating other tumor
813 types), the predicted treatment was not labeled as “EMPIRIC” and the case was instead evaluated
814 in context of the proven/suspected tumor type. In our analysis, we considered the TRUE group
815 as the concordant group, and FALSE and SOFT FALSE groups as the discordant group. We did
816 not include the EMPIRIC group, which is typically a more challenging patient population with
817 systematically worse outcomes [40].